Supplementary information for

"Strong bulk-surface interaction dominated in-plane anisotropy of electronic structure in GaTe"

Kang Lai†, Sailong Ju†, Hongen Zhu†, Hanwen Wang, Hongjian Wu, Bingjie Yang, Enrui Zhang, Ming Yang, Fangsen Li, Shengtao Cui, Xiaohui Deng, Zheng Han*, Mengjian Zhu*, Jiayu Dai*

†These authors contributed equally.

*Corresponding to Z.H. (email: vitto.han@gmail.com) or to M.Z. (email: zhumengjian11@nudt.edu.cn) or to J.D. (email: jydai@nudt.edu.cn).

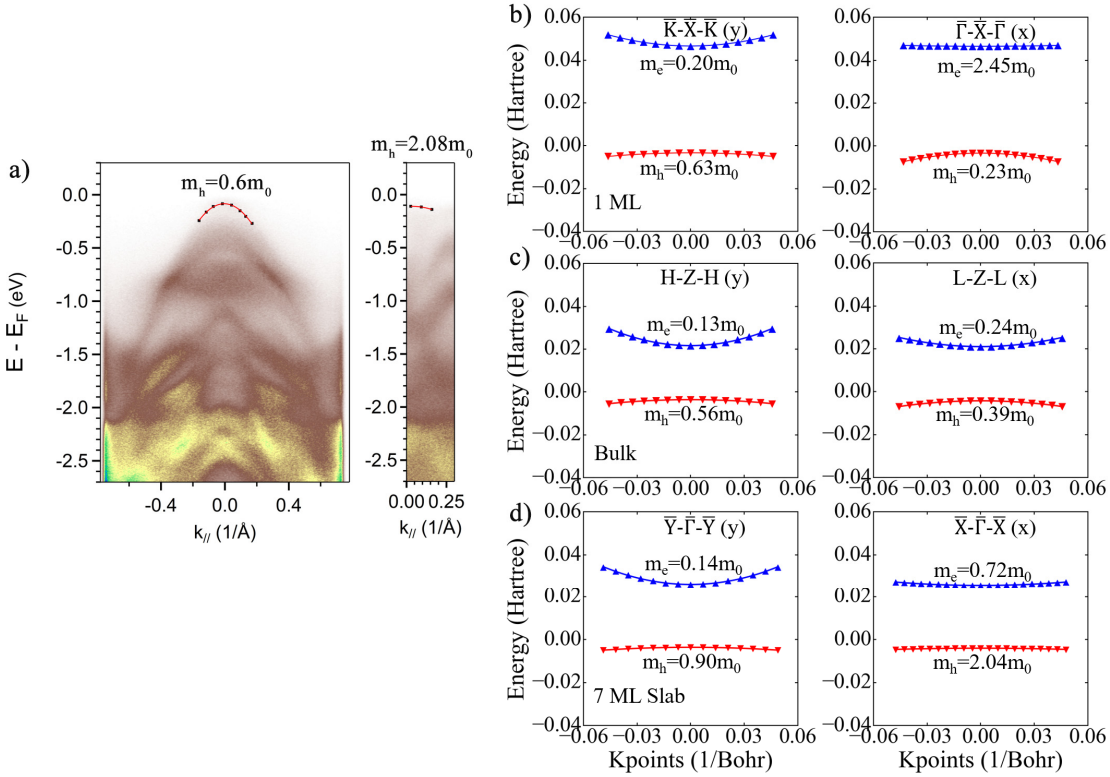

Supplementary Figure 1. Interpreting the anisotropic hole effective masses of GaTe obtained by ARPES. (a) Hole effective mass (m_h) of GaTe along y and x directions obtained by ARPES. **(b-d)** m_h and electron effective masses (m_e) along y and x direction for GaTe monolayer (1 ML), bulk and 7 ML slab configuration, respectively, which are predicted on the basis of band structure calculated by PBE+SOC method. These results are extracted by using a parabolic line fit**.**

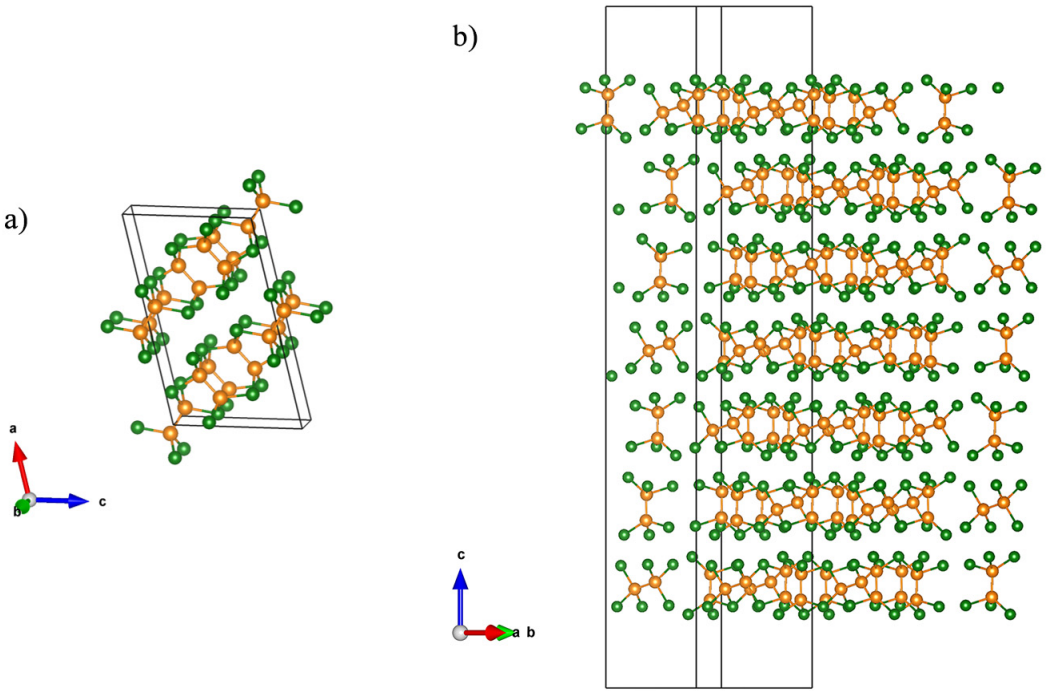

Supplementary Figure 2. Crystal structures of GaTe. (a) Bulk unit cell and **(b)** 7 ML slab configuration of GaTe. The orange and green balls represent Ga and Te atoms, respectively.

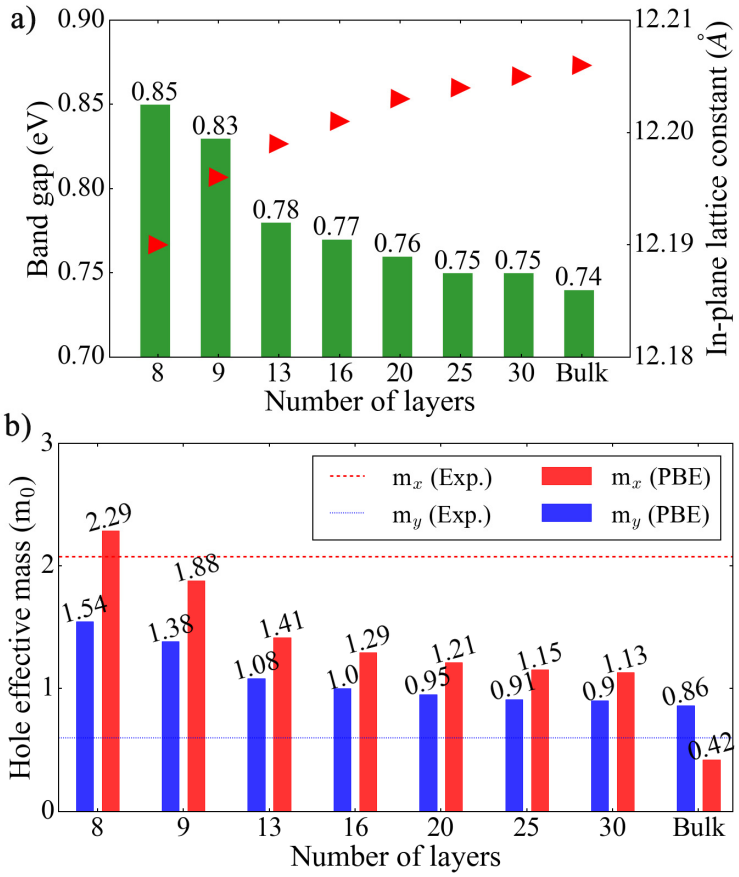

Supplementary Figure 3. Effect of quantum confinement on anisotropic band structure of GaTe. (a) In-plane lattice constants and band gaps evolution with number of layers. **(b)** Hole effective masses for x and y direction in units of free electron mass m_0 as a function of number of layers compared with experimental results.

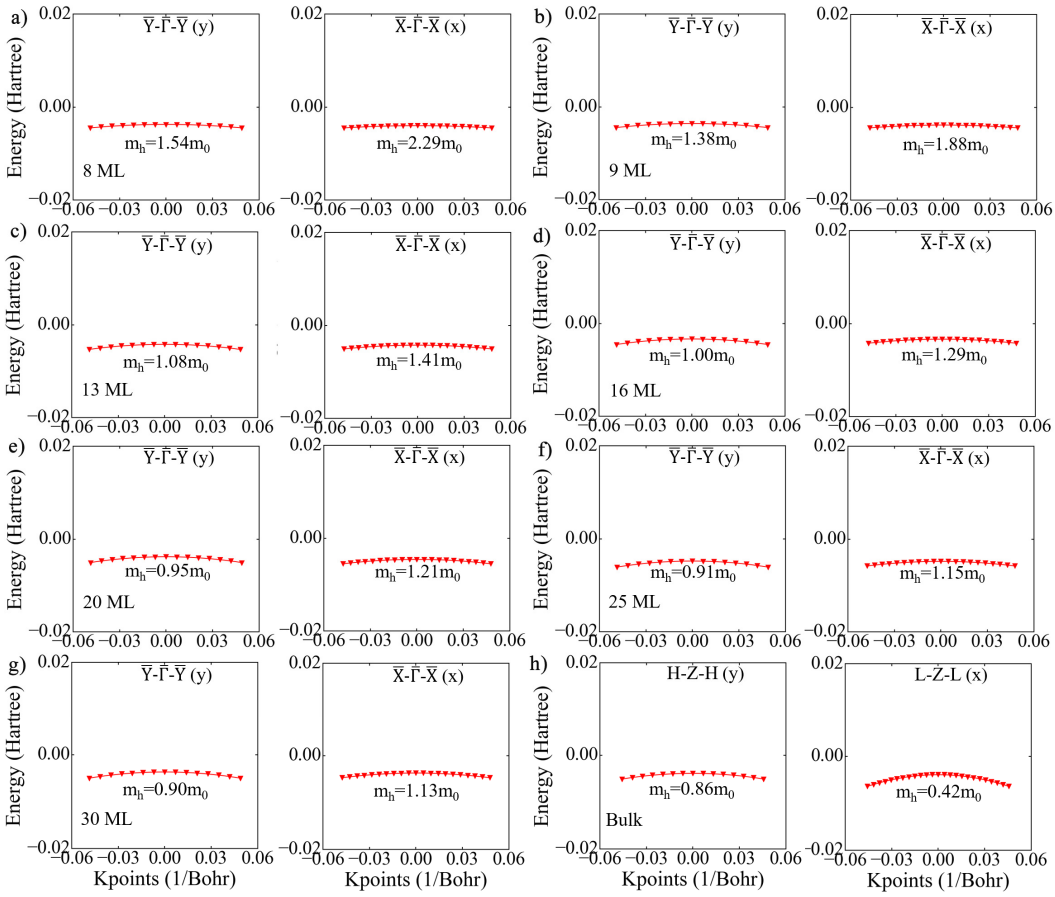

Supplementary Figure 4. Hole effective masses of multilayer GaTe. (a-g) Hole effective masses along x and y directions for GaTe with thickness of 8 ML, 9 ML, 13 ML, 16 ML, 20 ML, 25 ML and 30 ML. **(h)** Hole effective masses along x and y directions of infinite extended bulk GaTe. These results are obtained on the basis of band structure calculated by PBE functional.

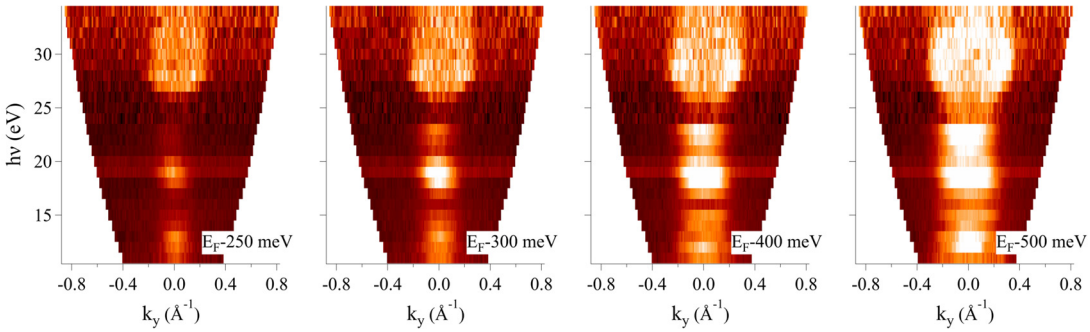

Supplementary Figure 5. The ARPES intensity near Fermi level as a function of the momentum k_y and the probing photon energy (11 to 34 eV).

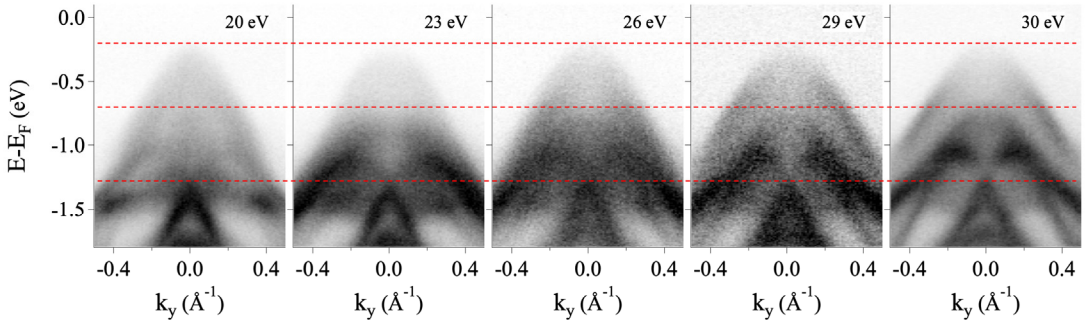

Supplementary Figure 6. The band dispersion along k_y direction using different photon energies.

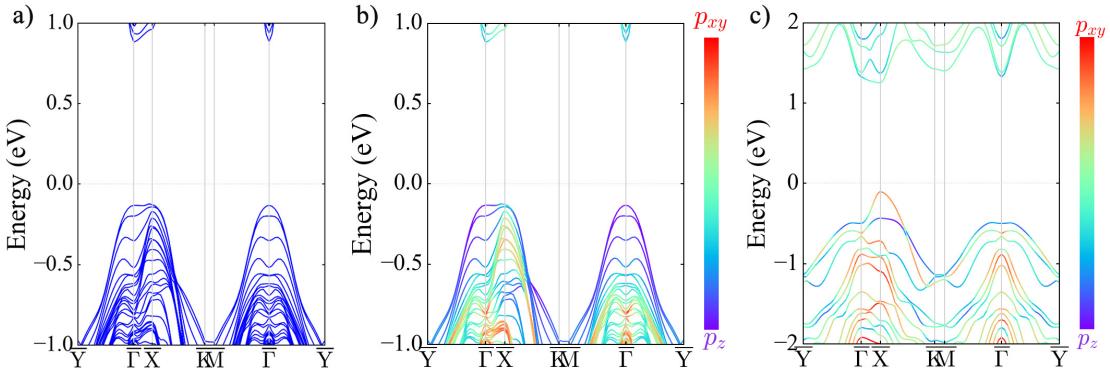

Supplementary Figure 7. Comparison between band structures for 7 ML GaTe with larger interlayer distances and 1 ML GaTe. (a-b) Band structure and orbital-projected band structure of 7 ML GaTe with larger interlayer distances. **(c)** Orbital-projected band structure of 1 ML GaTe.

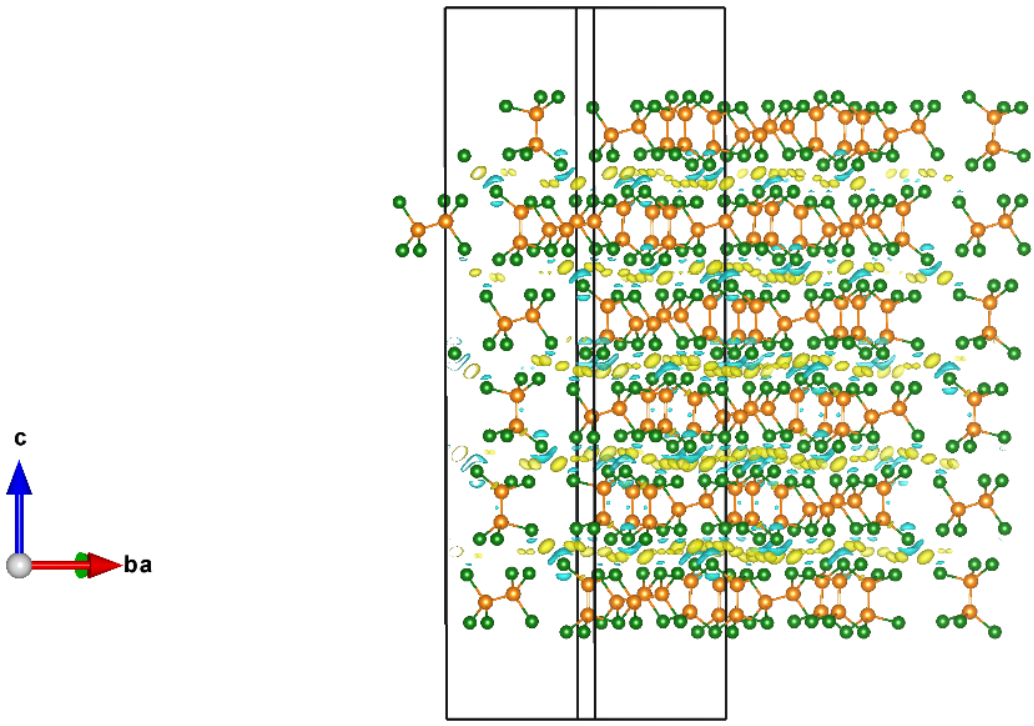

Supplementary Figure 8. Charge density difference Δρ between 6 ML and 1 ML GaTe, where Δρ=ρ(6layers)-ρ(monolayers). The isovalue is 0.002e/Å^3, and the yellow and blue represent gaining and losing electrons.

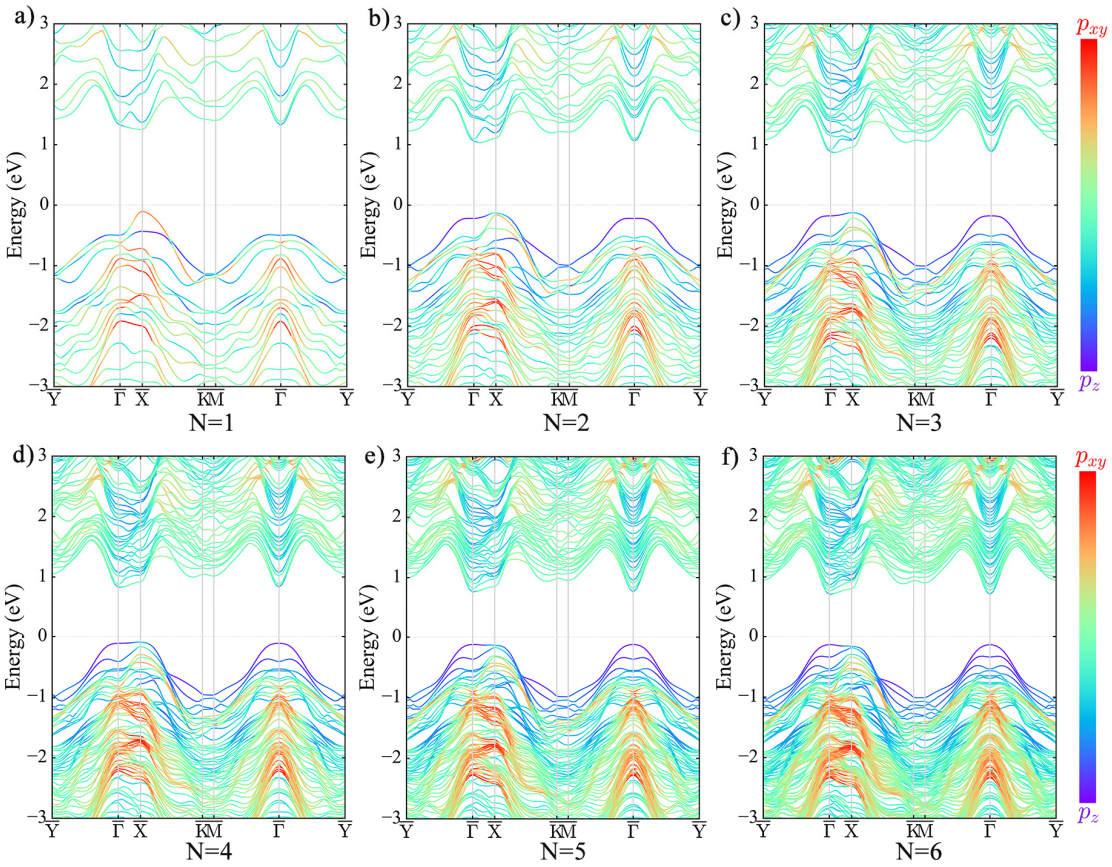

Supplementary Figure 9. Layer-dependent orbital-projected band structures of GaTe. **(a-f)** The p_{xy} and p_z orbital-projected band structures of GaTe in the dependence of number of layers (N).

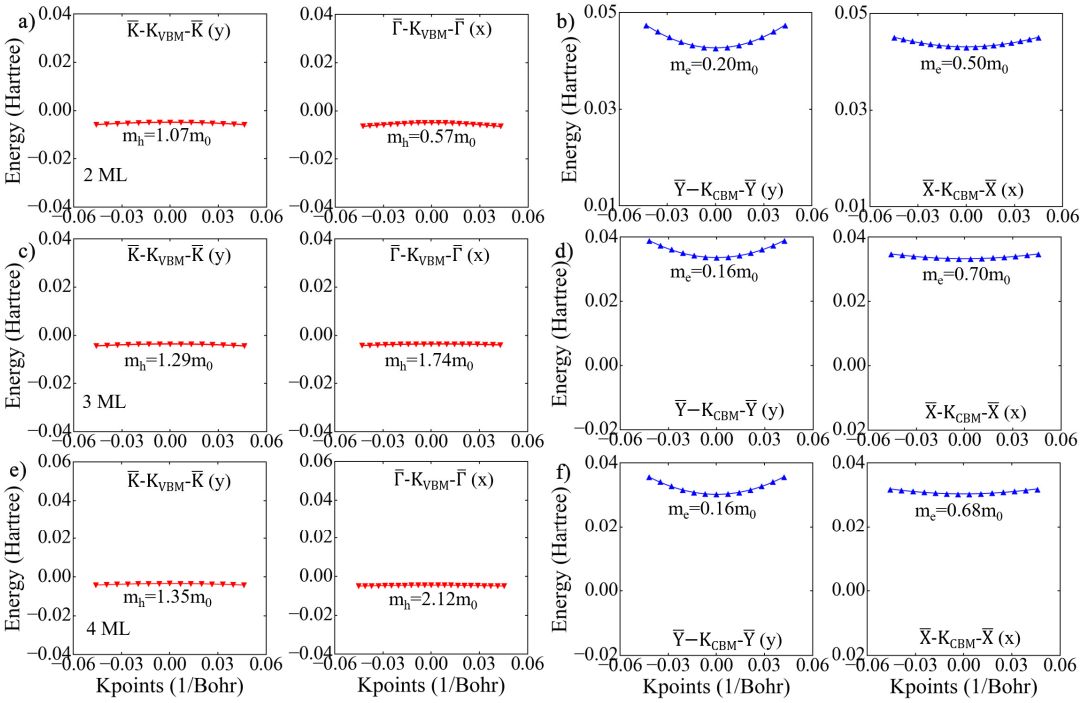

Supplementary Figure 10. Carrier effective mass of few-layer GaTe with indirect band gap. (a, c, e) Hole effective mass along y and x direction in units of free electron mass m_0 for 2ML, 3ML and 4ML GaTe, respectively. **(b, d, f)** Electron effective mass along y and x direction in units of free electron mass m_0 for 2ML, 3ML and 4ML GaTe, respectively. K_{VBM} and K_{CBM} denote the points that VBM and CBM located at, respectively.

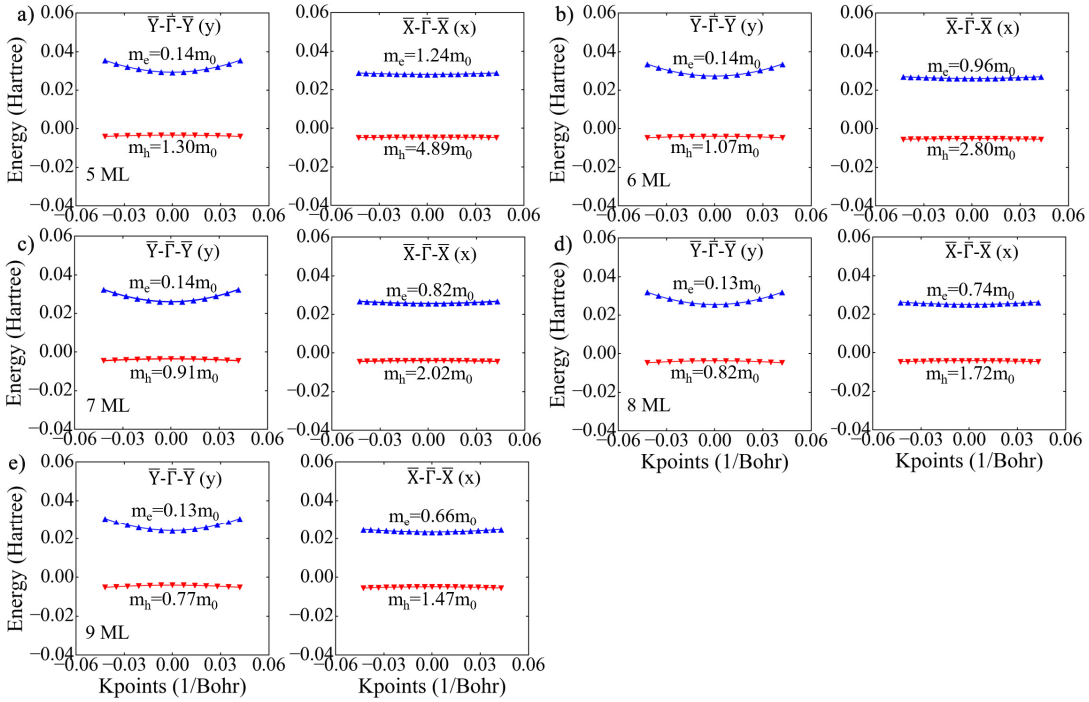

Supplementary Figure 11. Carrier effective mass of few-layer GaTe with direct band gap. (a-e) Hole and electron effective mass along y and x direction in units of free electron mass m_0 for 5ML, 6ML, 7ML, 8ML and 9ML GaTe, respectively.

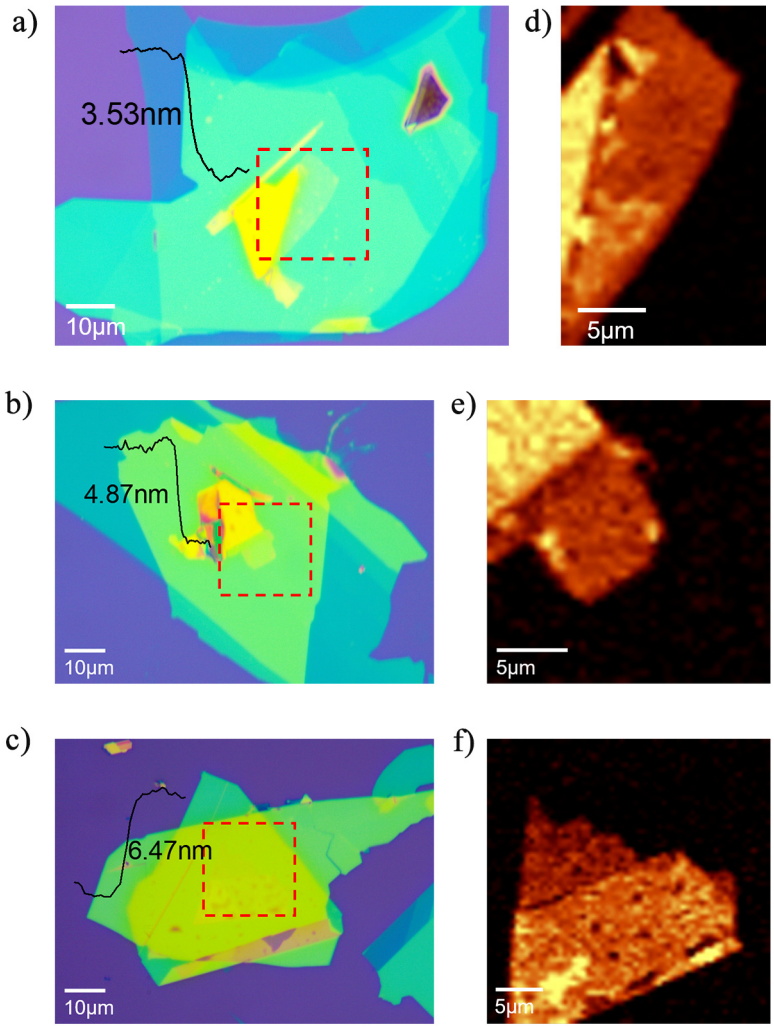

Supplementary Figure 12. Visualization of GaTe thin films encapsulated by h-BN. (a–c) Optical microscopy images and atomic force microscope height profiles of GaTe thin films. The red dashed square marks the area of AFM measurement and the following Raman imaging. **(d–f)** Corresponding Raman maps of integrated intensity of Raman mode at 115cm^{-1}.

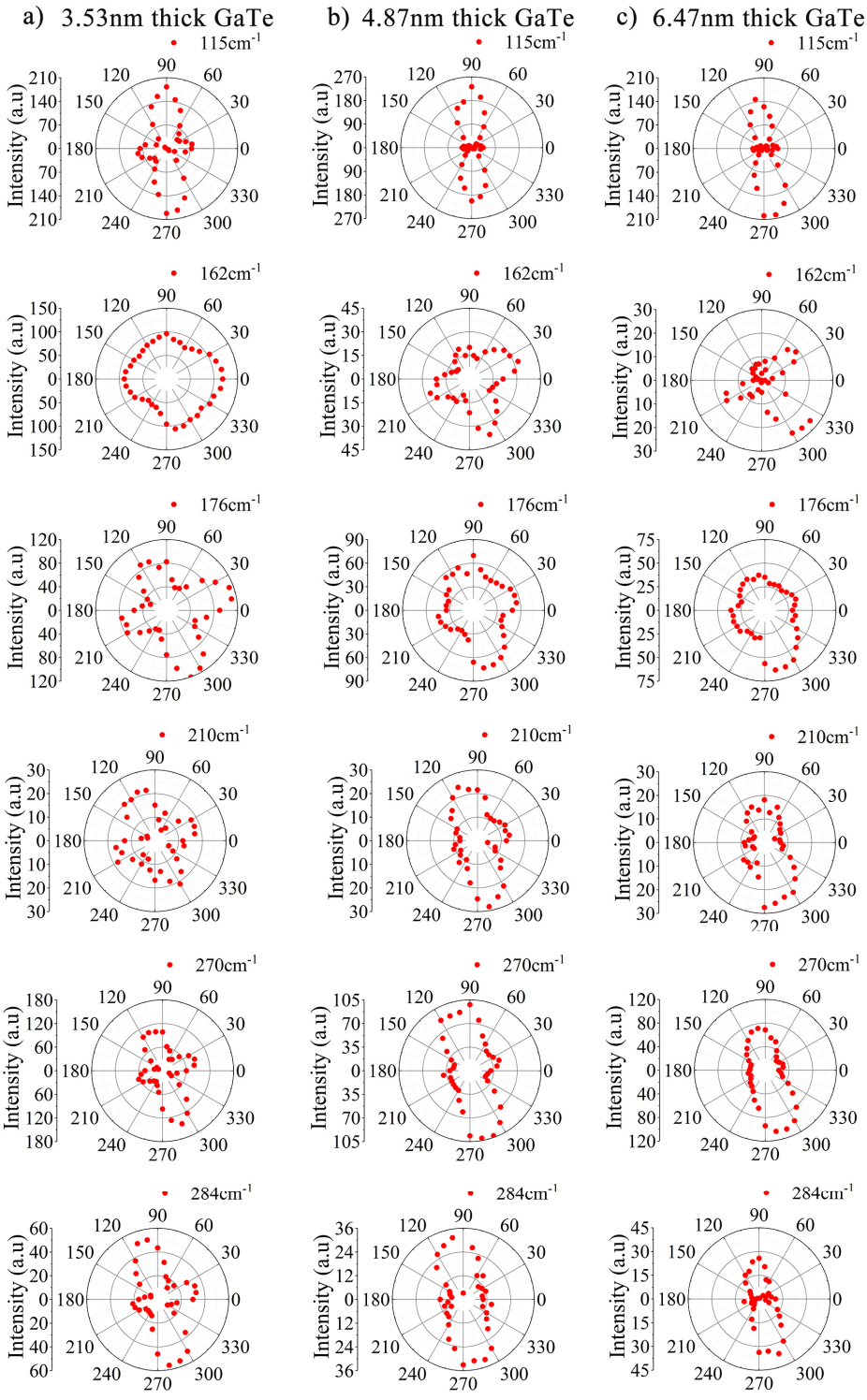

Supplementary Figure 13. The Raman intensity v.s. polarization angle for six types of Raman modes of GaTe thin films. (a-c) The Raman intensity polar plots of GaTe thin films with thickness of 3.53, 4.87 and 6.47 nm, respectively.

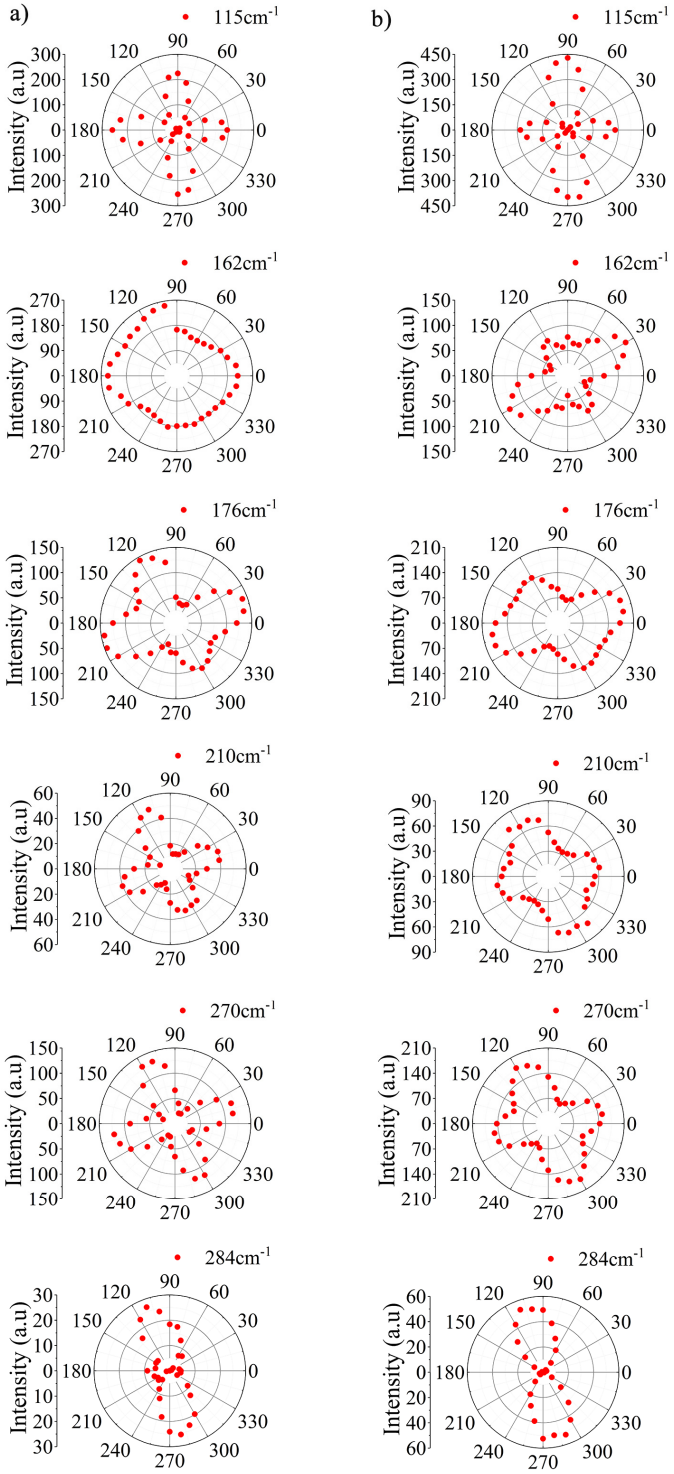

Supplementary Figure 14. The Raman intensity v.s. polarization angle for six types of Raman modes of GaTe bulk. (a, b) The Raman intensity polar plots of GaTe bulk as reference which the 3.53 and 4.87 nm GaTe thin flakes have the same in-plane orientation with, respectively.

	a	b	c	α	β	γ
Exp. [1]	17.404 Å	4.077 Å	10.456 Å	90°	90°	104.44°
PBE	18.885 Å	4.147 Å	11.097 Å	90°	90°	108.99°
optB88-vdW	17.622 Å	4.160 Å	10.614 Å	90°	90°	104.12°

Supplementary Table 1. Unit cell parameters of bulk GaTe, obtained using optB88-vdW and PBE functionals.

N	a(Å)	d1(Å)	d2(Å)	d3(Å)	d4(Å)	d5(Å)	d6(Å)	d7(Å)	d8(Å)
1	12.100	-	-	-	-	-	-	-	-
2	12.177	2.053	-	-	-	-	-	-	-
3	12.170	2.050	2.049	-	-	-	-	-	-
4	12.174	2.059	2.019	2.111	-	-	-	-	-
5	12.187	2.059	2.057	2.072	2.058	-	-	-	-
6	12.184	2.034	2.013	2.057	2.103	2.161	-	-	-
7	12.193	2.060	2.055	2.052	2.049	2.053	2.055	-	-
8	12.190	2.083	2.081	2.082	2.082	2.081	2.082	2.082	-
9	12.196	2.063	2.064	2.060	2.063	2.064	2.060	2.065	2.063

Supplementary Table 2. Unit cell parameters of GaTe with number of layers (N) from 1 to 9, obtained by optB88-vdW functional. In-plane lattice constant is denoted by a. The interlayer distances between different layers are denoted by d1, d2, d3, d4, d5, d6, d7 and d8 respectively.

Supplementary References

[1] Zhao, Q. et al. Thickness-induced structural phase transformation of layered gallium telluride. PCCP 18, 18719-18726 (2016).